United States Department of Agriculture

Evaluation of Modulus of Elasticity and Modulus of Rupture of Cross-Laminated Timber with Longitudinal Vibration NDE Techniques

Laurice Mara Spinelli Correa
Frederico José Nistal França
Rubin Shmulsky
R. Daniel Seale
Robert J. Ross
Christopher Senalik

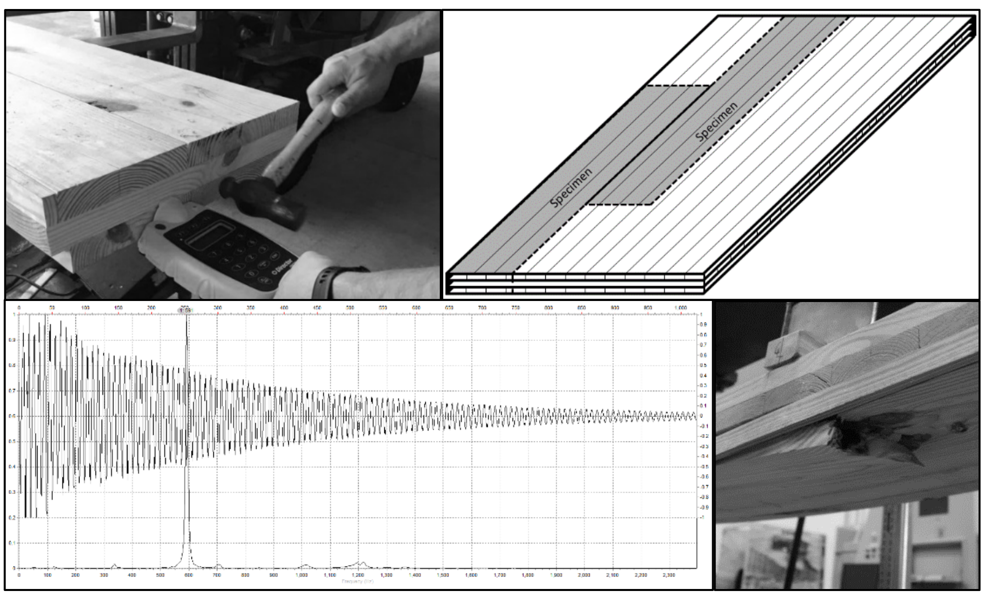

Forest Service | Forest Products Laboratory | Research Paper FPL–RP–714 | April 2022

Abstract

This paper presents research conducted to examine the potential of using longitudinal vibration techniques to evaluate the modulus of elasticity and strength of cross-laminated timber (CLT). Thirty-nine CLT panels were manufactured from southern pine dimension lumber in accordance with accepted manufacturing standards. Nominal 2 by 8 in. southern pine lumber specimens were used for the three-ply panels. A 10-ft-long specimen, having a 4.125- by 18-in. cross-section, was obtained from each panel. Weight and dimensions were determined for each specimen, and longitudinal vibration nondestructive evaluation techniques were used to determine frequency of oscillation and energy loss characteristics of the specimens. The dynamic modulus of elasticity was then determined. Each specimen was then tested to failure in a flatwise (third point) bending mode. Flatwise bending modulus of elasticity and strength (modulus of rupture) were determined. Excellent correlative relationships were observed between dynamic and flatwise bending moduli. A strong positive relationship was observed between the dynamic modulus and flatwise bending strength. Nondestructive testing of CLT panels is recommended for quality control protocols.

Keywords: CLT, MOE, MOR, SYP, longitudinal vibration, time domain, frequency domain, strength model

April 2022

Correa, Laurice Mara Spinelli; França, Frederico José Nistal; Shmulsky, Rubin; Seale, R. Daniel; Ross, Robert J.; Senalik, Christopher. 2022. Evaluation of modulus of elasticity and modulus of rupture of cross-laminated timber with longitudinal vibration NDE techniques. Research Paper FPL-RP-714. Madison, WI: U.S. Department of Agriculture, Forest Service, Forest Products Laboratory. 9 p.

A limited number of free copies of this publication are available to the public from the Forest Products Laboratory, One Gifford Pinchot Drive, Madison, WI 53726-2398. This publication is also available online at www.fpl.fs.fed.us. Laboratory publications are sent to hundreds of libraries in the United States and elsewhere.

The Forest Products Laboratory is maintained in cooperation with the University of Wisconsin.

Contents

Evaluation of Modulus of Elasticity and Modulus of Rupture of Cross-Laminated Timber with Longitudinal Vibration NDE Techniques

Laurice Mara Spinelli Correa, Doctoral Candidate
Frederico José Nistal França, Assistant Research Professor
Rubin Shmulsky, Head and Warren S. Thompson Professor of Wood Science and Technology
R. Daniel Seale, Warren S. Thompson Professor of Wood Science and Technology
Mississippi State University, Department of Sustainable Bioproducts, Starkville, Mississippi, USA

Robert J. Ross, Supervisory Research General Engineer
Christopher Senalik, Research General Engineer
USDA Forest Service, Forest Products Laboratory, Madison, Wisconsin, USA

Introduction

The use and production of mass timber products in the United States and North America have grown significantly in the past three years. More than 100 structures have been built using cross-laminated timber (CLT) and other mass timber panel products, with hundreds of additional projects under development (WoodWorks 2021). Primary markets include commercial and multifamily residential buildings, but interest in single-family homes and timber bridge decks is growing. Four CLT producers are currently operating in the United States, with at least five more manufacturing facilities announced or under construction. To support production, an American National Standard, Standard for Performance-Rated Cross-Laminated Timber PRG 320 (ANSI/APA 2019), was developed and approved through a consensus process. The original was published in 2017 and updated in 2018 and 2019. Delamination tests and visual quality inspection of panels are required for industrial mass production as part of an in-plant quality control program.

CLT is a multilayer wood composite material manufactured from structural lumber. Depending on how the properties of the lumber change or on which adhesive is used, its manufacture may adversely influence its performance. The abilities to detect the presence of delamination and to determine stiffness and strength of CLT are important in its production and in-service.

The wood nondestructive evaluation community has been investigating techniques to locate delamination in wood composite materials since the 1960s. One of the earliest efforts was that of Jayne (1965) and Suddarth (1965), who worked jointly on a study funded by the Department of Defense designed to investigate the possibility of using mechanical impedance to locate poorly bonded or debonded areas in the nose cones of Polaris missiles.

A variety of techniques have been investigated since then, with a significant effort aimed at investigating acoustic (stress wave, ultrasound) techniques in a variety of modes (through transmission, pulse echo, contact, noncontact). Most composite manufacturing facilities (oriented strandboard, particleboard, plywood) currently use some type of noncontact acoustic sensing system to monitor their products on-line. They specifically look for delamination, commonly referred to as “blows,” caused by excess steam buildup during the pressing operation. These systems are commercially available. They are designed for use in large production facilities. Portable equipment that utilizes the same concepts is widely available and used for inspection of wood structures around the world.

Several studies (Ross and Pellerin 1988, Vogt 1986) investigated the relationship between sound transmission (sound) and bending and tension strength of wood composites. Excellent correlative models were developed relating sound transmission properties and the strength of wood composites.

This research aims to develop (1) quality assurance procedures for monitoring the quality of mass timber and CLT after manufacturing and (2) techniques to assess mass timber in-service. Its objective was to investigate the use of a longitudinal vibration nondestructive technique to predict static bending properties of southern pine CLT panels. To achieve this,

- the longitudinal stress wave signal was recorded and analyzed,

- correlations between nondestructive testing (NDT) variables with CLT stiffness and strength were analyzed, and
- regression models were developed to predict bending MOE and MOR.

Materials and Methods

Twenty-four 8- by 16-ft (2.43- by 4.88-m) three-ply commercial panels were procured. The panels were made per PRG-320 from 2 by 8 (nominal) No. 2 southern yellow pine (SYP) lumber and with core layer from No. 3 SYP. Table 1 shows the design values for lamination in longitudinal layers. Per ANSI / APA PRG 320-2019, this material is classified as V3.

Twenty-eight specimens were tested. One test specimen was ripped from each of 20 panels. From the four panels remaining, two test specimens were ripped (Fig. 1). Each specimen was cut from the original CLT panel and was approximately 4.125 in. (105 mm) thick, 18 in. (457 mm) wide, and crosscut to 120 in. (3.05 m) long.

Final dimensions of each specimen were measured, and weight was recorded for density estimation. Specimen density was determined using the bulk weight and bulk volume. Percentage moisture content (MC) was determined using a Model MMC 220 electric moisture meter (Wagner Meters, Rogue River, Oregon). Longitudinal vibration signal (also called longitudinal stress wave signal) was obtained and recorded for every specimen using a Hitman HM 200 tool (Fibre-gen, Ltd., Christchurch, New Zealand).

An impact was applied on each test specimen in the longitudinal direction per ASTM E1876 (ASTM 2015). A consistent impact was done using a hammer, trying to ensure similar level of impact energy for all specimens. Which ply was impacted had no effect because panels vibrated as a single piece. The direction of the wave motion was in the same direction as the longitudinal vibration mode. Dynamic modulus of elasticity (MOE) was calculated for the information collected by the longitudinal vibration tool (Fig. 2) by applying

$$E_L = \rho v^2 = \rho (2Lf)^2 \quad (1)$$

where E_L is dynamic MOE (MPa), ρ is density (kg m^{-3}), L is length of the piece (m), f is first harmonic longitudinal vibration frequency (Hz), and v is wave velocity (m s^{-1}).

A linear regression analysis was conducted to determine the values for the unknown empirical constants, K and x, for flexural MOE and modulus of rupture (MOR), following the procedure described by Senalik and Ross (2015). The model was implemented using the dynamic MOE as the sole nondestructive variable:

$$\ln P = \ln K + x \ln E_d \quad (2)$$

where P is the property being estimated, K is a constant, and E_d is dynamic MOE.

The Hitman HM 200 software converts the time-domain into a frequency-domain signal through a fast Fourier transform. The software output permits visualization of the time-domain and frequency-domain graph (Fig. 3).

Identification of the fundamental frequency was possible for every CLT specimen. A consistent longitudinal strike (hammer hit) on the cross section excited the CLT specimen

Table 1—Design values (MPa) for laminations in longitudinal layers, per V3

F_b[a]	Characteristic value[b]	F_b for No. 2 2 by 8 lumber[c]	MOE[c]
5.17	10.86	6.38	9,653

[a] PRG-320, table A1.
[b] PRG-320, table 1. (Note: Fb = Characteristic value/2.1).
[c] SPIB 2014

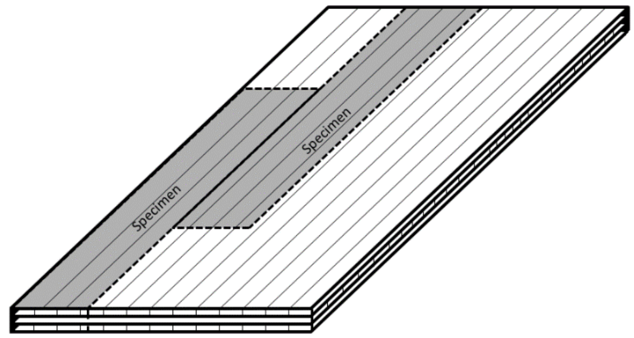

Figure 1—Three-ply CLT panel and specimens rip scheme.

Figure 2—Longitudinal vibration evaluation of a three-ply CLT panel using a Hitman HM 200 tool.

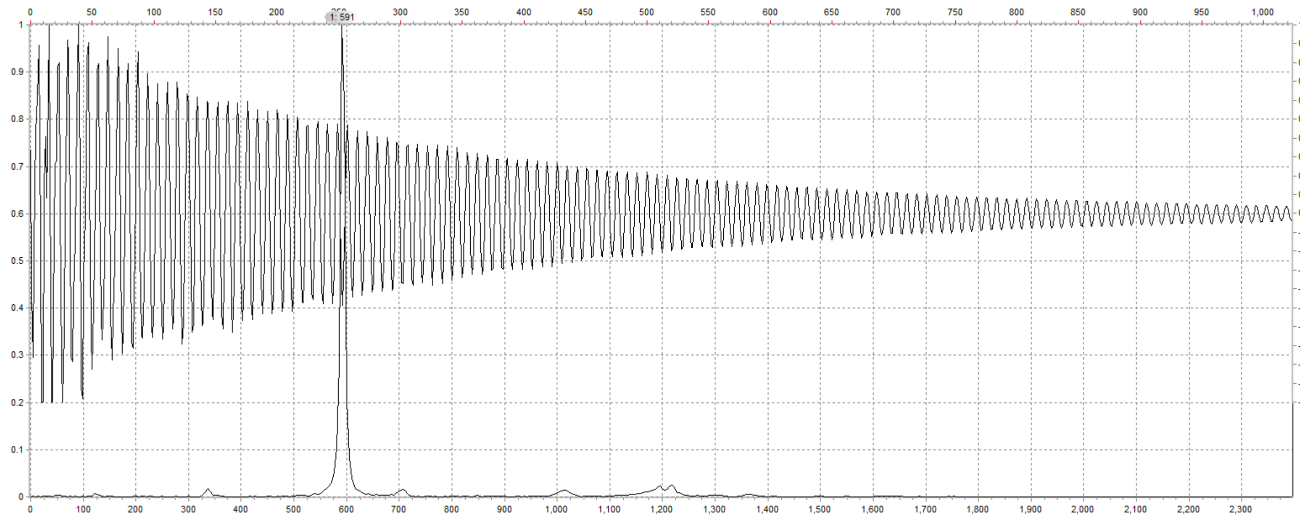

Figure 3—Longitudinal vibration signal output from the Hitman HM 200.

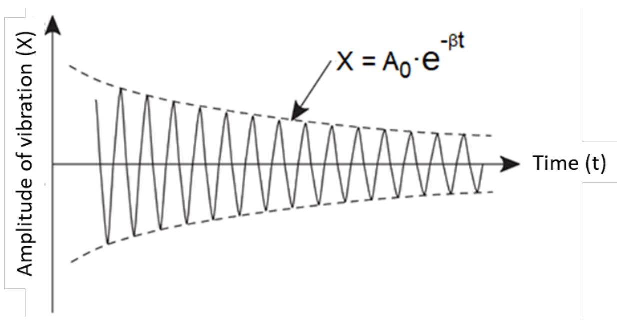

Figure 4—Logarithmic decrement exponential (ß) over the time domain signal.

and generated the fundamental frequency. Note that the fundamental frequency is very prevalent, and the sub-sequential harmonics were not detectable for most specimens.

After the acoustic signals were recorded for all specimens, the sample was tested destructively by third point bending over a 9.5-ft (2.9-m) span. This setup provided a span-to-depth ratio of 27.6 and consistent with PRG-320 (ANSI/APA 2019) guidance "specimen width not less than 12 inches (305 mm) and the on-center span equal to approximately 30 times the specimen depth for the tests in the major strength direction... ." Flexure testing was conducted on each specimen using a four-point bending setup per ASTM D 5456 (ASTM 2017a).

Evaluation of energy loss (damping) was conducted. The calculation of the frames' hysteresis damping using the logarithmic decrement (LD) method collected from longitudinal vibration described in Senalik et al. (2020a). LD (recorded in the database for every piece) is calculated from the exponential covering curve over the time-domain sinusoidal curve (Fig. 4), given by

$$\mathrm{LD} = \beta t \quad (3)$$

where β is the parameter of the exponential covering curve and t is period of time (s) (the inverse of frequency in Hz).

An approach following the one described by Senalik et al. (2020b) was followed. Preliminary assessment focused on two regions of the time domain signal: the earliest arrival of the signal and late in the signal when the wave energy begins to attenuate. A CLT specimen should have disruption to the wave as it travels due to features such as knots and slope of grain; the signal will be disrupted through reflection, mode conversion, and increased attenuation.

The areas under the curve in the time-domain signal (TDA) and the frequency-domain signals (FDA) in specific segments were calculated. The region between 300 and 400 µs was chosen for measuring the area in the time-domain signal (Fig. 5, top). The natural frequency peak was the second area measured for each specimen (Fig. 5, bottom).

Statistical analyses and associated graphs were completed according to ASTM D2915 (ASTM 2017b) using SAS version 9.4 (SAS 2013). Bivariate correlations among variables were evaluated. The variables MOE and MOR were used as multiple linear functions of density and NDT properties. To predict MOE and MOR using NDT variables, a stepwise procedure was used for fitting models. For each relationship obtained, the coefficient of correlation (R) and coefficient of determination (R^2) were calculated. The following equations were used to predict MOE and MOR:

$$\mathrm{MOE} = f(\mathrm{dMOE, LD, TDA, FDA}) + \varepsilon_1 \cdots \quad (4)$$

$$\mathrm{MOR} = f(\mathrm{dMOE, LD, TDA, FDA}) + \varepsilon_2 \cdots \quad (5)$$

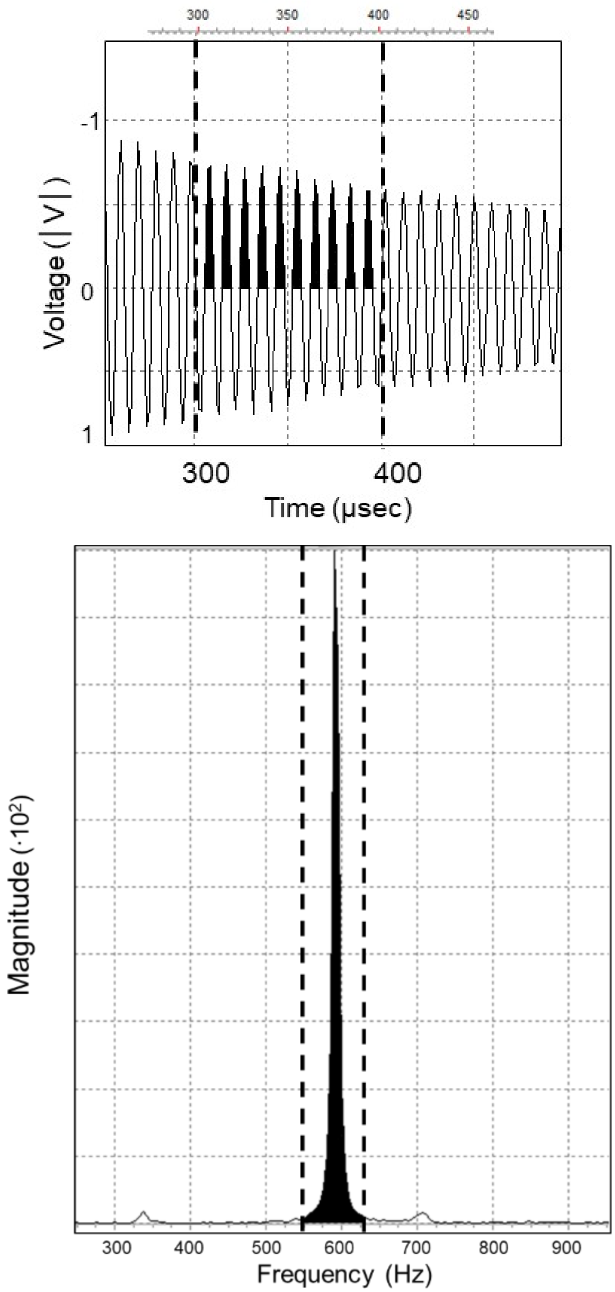

Figure 5—Area under the curve for (top) time-domain signal between 300 and 400 µs and (bottom) natural frequency peak between 550 and 620 Hz.

Results and Discussion

Table 2 shows result summaries for each physical and mechanical property for the CLT specimens tested. Overall means for MOE and MOR were 8,057 and 34.87 MPa, respectively. The values found in this study showed a narrow range for both properties compared with those of structural lumber. Low coefficient of variation (2.63%) was found for density among specimens. Dynamic MOE values found in this study were lower than the related static MOE values because of the low longitudinal vibration velocities found in CLT compared with those of 2 by 8 SYP lumber (~4,500 m s^{-1}) and explained by the lower length-to-width ratio (6.6 to 1).

Comparing the static MOE values found in this study with the current design value for 2 by 8 SYP No. 2 lumber (9,653 MPa), the results show that MOE values for CLT specimens were lower than the published design value (American Wood Council 2018). The overall MOR was lower than the values reported for southern pine lumber by other authors: Dahlen et al. (2014; 40.7 MPa) for different No. 2 lumber sizes; Yang et al. (2017; 38.26 MPa) for No. 2 2 by 4; França et al. (2020; 39.60 MPa) for No. 2 2 by 8.

Bivariate correlations among the variables under investigation are presented in Table 3. For MOR, the highest correlation was seen for dMOE ($R = 0.63$). Logarithmic decrement had a negative correlation with MOE ($R = –0.43$) and MOR ($R = –0.26$), where higher decrement is related to weaker pieces. Similar LD results were found by Divós and Sismándi-Kiss (2010) for spruce, larch, and pine structural lumber. França et al. (2019) found an $R = –0.22$ studying southern pine 2 by 4 and 2 by 6 lumber.

Frequency-domain area had a negative correlation with MOR ($r = –0.57$). It was noticed that narrow base peak contributes to a smaller fundamental frequency area. Time-domain area exhibited a positive correlation with MOR ($r = 0.62$). Higher quality pieces had greater area under the time-domain curve segment. Figure 6 shows linear regression plots for three-ply SYP CLT showing bending MOE vs dynamic MOE and bending MOR vs dynamic MOE.

The R^2 for MOE prediction was 0.90, showing an increase when compared to lumber resulting from the homogeneity of the panels. Yang et al. (2015) studying the prediction of MOE of southern pine dimensional lumber using longitudinal vibration waves found R^2 values ranging from 0.77 to 0.86. França et al. (2020) studying SYP No. 2 lumber found a higher $R^2 = 0.76$ and 0.77 (2 by 8 and 2 by 10, respectively) using the Director HM 200. The results found in this study emphasize the potential of longitudinal vibration wave techniques to estimate MOE.

Although the results for predicting static MOE are favorable and accurate ($R^2 = 0.90$), the relationships for MOR are still limited (Fig. 6). The R^2 for MOR prediction found in this study was 0.33. Yang et al. (2017) found R^2 values for dMOE and bending MOR ranging from 0.23 to 0.28. França et al. (2020) studying SYP No. 2 lumber found $R^2 = 0.15$ and 0.20 (2 by 8 and 2 by 10, respectively) using the Director HM 200.

Two possible outliers were detected in Figure 6b. Further evaluation of the specific specimens led to the detection of knots on the tension surface of the specimen (Fig. 7). Although the knots affected panel performance, the size of

Table 2—Bending modulus of elasticity (MOE), modulus of rupture (MOR), density, stress wave velocity, and dynamic MOE values for CLT specimens[a]

	MOE (MPa)	MOR (MPa)	Density (kg m^{-3})	Velocity (m s^{-1})	dMOE (MPa)	LD	FDA	TDA
Average	8,057	34.87	535	3,563	6,800	0.044	6,575	940
Minimum	5,755	23.07	503	3,110	4,865	0.035	4,444	197
Maximum	10,277	44.90	561	3,940	8,600	0.055	9,541	1817
COV (%)	12.46	14.67	2.63	5.22	12.09	11.33	15.86	57.07

[a] COV, coefficient of variation; dMOE, dynamic modulus of elasticity; LD, logarithmic decrement; FDA, frequency-domain area; TDA, time-domain area.

Table 3—Pearson's bivariate correlation (*r*) among modulus of elasticity (MOE), modulus of rupture (MOR), density, longitudinal stress wave velocity, dynamic MOE, logarithmic decrement, frequency-domain area, and time-domain area for the tested CLT sample[a]

	MOE	MOR	Density	Velocity	dMOE	LD	FDA	TDA
MOE (MPa)	1	0.58 (<0.01)	0.85 (<0.01)	0.90 (<0.01)	0.95 (<0.01)	–0.43 (0.02)	–0.50 (<0.01)	0.61 (<0.01)
MOR (MPa)		1	0.41 (0.03)	0.57 (<0.01)	0.63 (<0.01)	–0.26 (0.18)	–0.57 (<0.01)	0.62 (<0.01)
Density (kg/m^3)			1	0.67 (<0.01)	0.75 (<0.01)	–0.37 (0.06)	–0.38 (0.05)	0.47 (0.01)
Velocity (m/s)				1	0.98 (<0.01)	–0.50 (<0.01)	–0.48 (0.01)	0.48 (0.01)
dMOE (Mpa)					1	–0.48 (<0.01)	–0.50 (<0.01)	0.54 (<0.01)
LD						1	0.18 (0.35)	–0.27 (0.16)
Frequency-domain area							1	–0.72 (<0.01)
Time-domain area								1

*dMOE, dynamic modulus of elasticity; LD, logarithmic decrement; FDA, frequency-domain area; TDA, time-domain area.

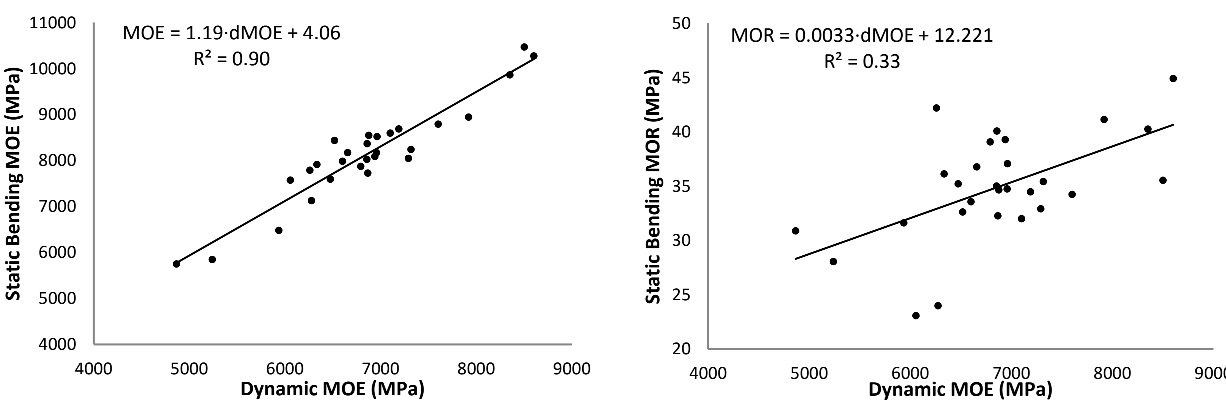

Figure 6—Linear regression plots for three-ply SYP CLT showing (left) bending MOE vs dynamic MOE and (right) bending MOR vs dynamic MOE.

Figure 7—Static bending failure due to presence of knot.

the knots are accepted in visually No. 2 graded lumber. The presence of knots on the tension face reduced the static bending strength values of the two specimens. Moreover, higher grade lumber on outer layers is recommended and would increase strength values of CLT panels.

The natural logarithmic relationship between predicted bending MOE and static bending MOE is shown in Figure 8 (left). Data from this study were compared with data of Ross and Pellerin (1988) from a wide range of composite panels. The $R^2 = 0.93$ value from the composite specimens was slightly higher than that of the CLT specimens ($R^2 = 0.90$). It can be concluded that the CLT specimens fit in the original MOE composite model from Ross and Pellerin (1988) reconstructed by Senalik and Ross (2015).

The relationship between predicted natural logarithmic MOR and bending MOR from the CLT specimen testing is shown in Figure 8 (right). Once again, the CLT specimens fit in the original MOR composite model from Ross and Pellerin (1988). However, the $R^2 = 0.33$ value from the CLT specimens was significantly lower than that of the composite specimens ($R^2 = 0.89$) from Ross and Pellerin (1988).

After evaluating the potential of dMOE on CLT stiffness and strength prediction, more nondestructive variables exhibiting potential use were added to the models to improve the prediction of MOE and MOR. Several studies showed the benefit of combining different grading variables (Diebold et al. 2000, Denzler et al. 2005, Hanhijarvi and Ranta-Maunus 2008, França et. al. 2019).

To determine the best-fit multiple regression equation, a stepwise regression approach was employed. Tables 4 and 5 show the regression model, coefficient of determination (R^2), standard error, and improvement of the linear regression for MOE and MOR on CLT sample. Time-domain area was the most significant secondary variable to predict MOE ($R^2 = 0.91$), adding an improvement of 5.33%.

The combination of dMOE with TDA + FDA, and TDA + FDA + LD presented slightly higher R^2 (0.91 and 0.92, respectively) but were not significant. In addition, the combination of these variables resulted in higher standard error when compared to dMOE + FDA model (Table 4).

Logarithmic decrement did not support the MOE and MOR prediction ($R^2 = 0.90$ and 0.33, respectively). Time-domain area exhibited a potential increase of 8.52% when combined with dMOE ($R^2 = 0.46$). The combination of all NDT variables slightly improved the regression model ($R^2 = 0.48$). However, the model was not significant (Table 5).

The result shows that the capability of prediction can be improved when two or more variables are added to the model. The result agrees with Senalik et al. (2020b), who found an increase in R^2 from 0.52 to 0.71 testing southern pine lumber pieces. The regression equations with the best models to predict MOE and MOR are shown in Table 6. Models with independent variables whose addition did not improve the model are not shown.

Figure 9 shows linear regression plots for three-ply SYP CLT using the models from Table 6. Predicted MOE using the generated model slightly improved the MOE estimation (from $R^2 = 0.90$ to $R^2 = 0.91$). In contrast, using two nondestructive variables substantially improved the prediction of the bending MOR ($R^2 = 0.33$ to $R^2 = 0.46$).

Conclusions

- Longitudinal vibration dynamic modulus of elasticity exhibited a high correlation with bending properties of CLT.
- Longitudinal vibration can be used to evaluate bending properties of CLT panels.
- The presence of knots on the outer layers of panels affected the strength the panels. Therefore, lumber with higher quality should be recommended for external layers.
- The addition of frequency-domain area in the regression model improved the MOE prediction.
- The addition of time-domain area in the regression model improved the MOR prediction.
- NDT evaluation of CLT panels is recommended for quality control protocols.

Acknowledgments

This research was funded by a grant from USDA Forest Service. This publication is a contribution and is approved as journal article SB 1044 of the Forest and Wildlife Research Center, Mississippi State University.

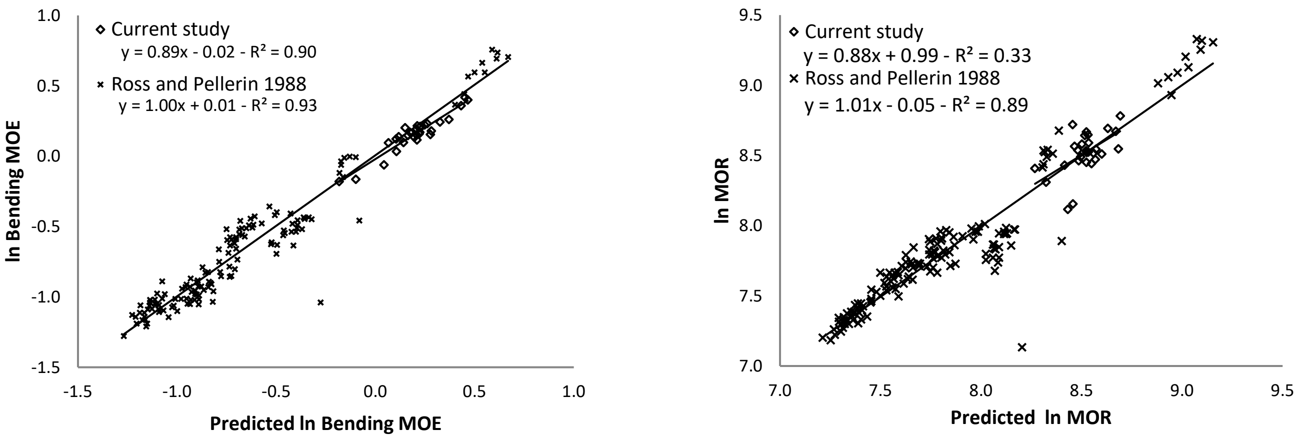

Figure 8—Natural logarithm of (left) predicted bending MOE vs bending MOE and (right) predicted MOR vs bending MOR.

Table 4—Modulus of elasticity (MOE) regression model, coefficient of determination (R^2), *p*-value, standard error of the estimate, and improvement of the linear regression[a]

Predictors	R^2	*p*-value	Standard error (MPa)	Improvement (%)[b]
dMOE	0.90	<0.001	346.9	—
dMOE + LD	0.90	0.042	352.7	–1.67
dMOE + FDA	0.90	0.038	351.3	–1.27
dMOE + TDA	0.91	0.021	328.4	+5.33
dMOE + TDA + FDA	0.91	0.052	331.3	NS
dMOE + TDA + FDA + LD	0.92	0.061	336.4	NS

[a] NS, not significant; dMOE, dynamic modulus of elasticity; LD, logarithmic decrement; FDA, frequency-domain area; TDA, time-domain area.
[b] Improvement (%) is in reference to the single predictor dMOE.

Table 5—Modulus of rupture (MOR) regression model, coefficient of determination (R^2), *p*-value, standard error of the estimate, and improvement of the linear regression[a]

Bending strength (MOR)	R^2	*p*-value	Standard error (MPa)	Improvement (%)[b]
dMOE	0.33	<0.0001	4.11	—
dMOE + LD	0.33	0.062	4.19	NS
dMOE + FDA	0.44	0.035	3.84	+6.57
dMOE + TDA	0.46	0.046	3.76	+8.52
dMOE + TDA + FDA	0.48	0.058	3.77	NS
dMOE + TDA + FDA + LD	0.48	0.089	3.85	NS

[a] NS, not significant; dMOE, dynamic modulus of elasticity; LD, logarithmic decrement; FDA, frequency-domain area; TDA, time-domain area.
[b] Improvement (%) is in reference to the single predictor (dMOE).

Table 6—Linear regression models with the largest coefficient of determination (R^2) and smallest error of estimate (μ) for dependent variables modulus of elasticity (MOE) and modulus of rupture (MOR)

	β_0	β_1	β_2	μ	R^2	Durbin-Watson
MOE = $\beta_0 + \beta_1$·dMOE + TDA	388	1.09	0.27	328	0.91	2.26
MOR = $\beta_0 + \beta_1$·dMOE + TDA	17.6	0.002	0.004	3.76	0.46	1.45

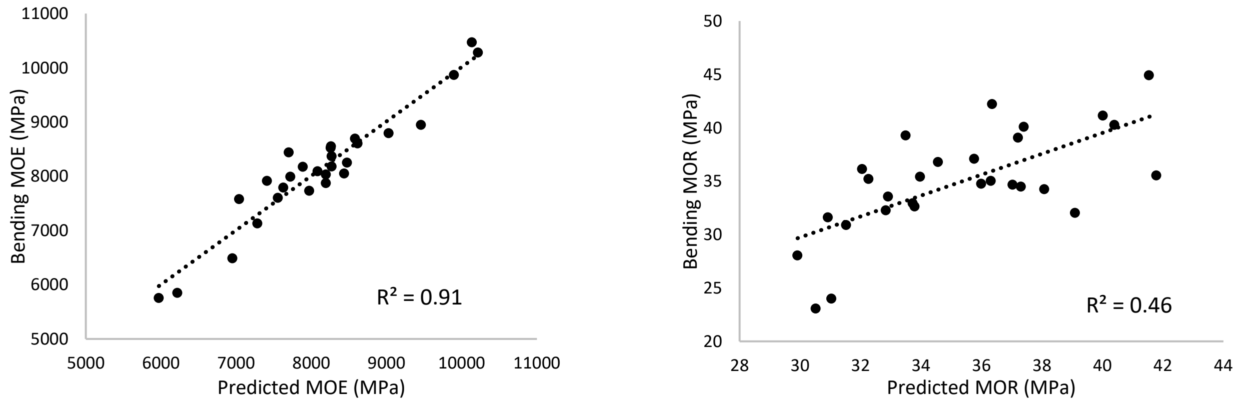

Figure 9—Linear regression plots (from Table 6) for three-ply SYP CLT showing (left) predicted MOE vs bending MOE and (right) predicted MOR vs bending MOR.

Literature Cited

ANSI/APA. 2019. 2018. PRG 320-2019. Standard for performance-rated cross-laminated timber. Tacoma, WA: APA–The Engineered Wood Association.

ASTM. 2015. E1876: Standard test method for dynamic Young's modulus, shear modulus, and Poisson's ratio by impulse excitation of vibration. West Conshohocken, PA: American Society for Testing and Materials.

ASTM. 2017a. D5456: Standard specification for evaluation of structural composite lumber products. West Conshohocken, PA: American Society for Testing and Materials.

ASTM. 2017b. D2915: Standard practice for sampling and data-analysis for structural wood and woodbased products. West Conshohocken, PA: American Society for Testing and Materials.

American Wood Council. 2018. National Design Specification (NDS) Supplement: Design Values for Wood Construction 2018 Edition. Leesburg, VA. May 2018.

Dahlen, J.; Jones, P.D.; Seale, R.S.; Shmulsky, R. 2014. Bending strength and stiffness of wide dimension southern pine No. 2 lumber. European Journal of Wood and Wood Products. 72(6): 759–768.

Denzler, J.; Diebold, R.; Glos, P. 2005. Machine strength grading—commercially used grading Machines—current developments. In: Proc., 14th international symposium on nondestructive testing of wood: 9–16.

Diebold, R.; Schleifer, A.;\, Glos, P. 2000. Machine grading of structural sawn timber from various softwood and hardwood species. In: Proc., 12th international symposium on nondestructive testing of wood: 139–146.

Divós, F.; Sismándi-Kiss, F. 2010. Strength grading of structural lumber by portable lumber grading—effect of knots. In: The future of quality control for wood & wood products. 4–7 May 2010, Edinburgh, Final Conference of COST Action E53.

França, F.J.N.; Seale, R.D.; Shmulsky, R.; França, T.S.F.A. 2019. Modelling mechanical properties of 2 × 4 and 2 × 6 southern pine lumber: longitudinal vibration and visual characteristics. Forest Products Journal. 68(3): 286–294.

Franca, F.J.N.; Franca, T.S.F.A.; Seale, R.D.; Shmulsky, R. 2020. Nondestructive evaluation of 2 by 8 and 2 by 10 southern pine dimensional lumber. Forest Products Journal. 70(1): 79–87.

Hanhijärvi, A.; Ranta-Maunus, A. 2008. Development of strength grading of timber using combined measurement techniques—report of the Combigrade-project—phase 2. Espoo, Finland: VTT Publications 686.

Jayne, B.A. 1965. The concept of mechanical impedance and its application to nondestructive testing. In: Proceedings, second nondestructive testing of wood symposium. Spokane, WA: Washington State University: 245–266.

Ross, R.J.; Pellerin, R.F. 1988. NDE of wood-based composites with longitudinal stress waves. Forest Products Journal. 38(5): 39–45.

SAS. 2013. SAS version 9.4. Cary, NC: SAS Institute Inc.

Senalik, C.; Ross, R.J. 2015. Predicting plywood properties with wood-based composite models. In: Proceedings: 19th international nondestructive testing and evaluation of wood symposium. General Technical Report FPL–GTR–239. Madison, WI: USDA Forest Service, Forest Products Laboratory.

Senalik, C.; França, F.J.N.; Seale, R.D.; Ross, R.J.; Shmulsky, R. 2020a. Estimating lumber properties with acoustic-based technologies—part 1: modeling acoustic (stress) wave behavior in clear wood and lumber. Wood and Fiber Science. 52(4): 380–389.

Senalik, C.; França, F.J.N.; Seale, R.D.; Ross, R.J.; Shmulsky, R. 2020b. Estimating lumber properties with acoustic-based technologies—part 2: ultimate tension stress estimation from time- and frequency-domain parameters. Wood and Fiber Science. 52(4):3 90–399.

SPIB. 2014. Standard grading rules for southern pine lumber, table 1-c-structural light framing, structural joists and planks, and studs—2" to 4" thick (8"-wide only). Pensacola, FL: Southern Pine Inspection Bureau.

Suddarth, S.A. 1965. Detection of adhesive bond defects in the Polaris missile nose fairing through mechanical impedance measurements. In: Proceedings, second nondestructive testing of wood symposium Spokane, WA: Washington State University: 267–287.

Vogt, J.J. 1986. Longitudinal stress waves as predictors of internal bond strength. In: Proceedings, 12th international particleboard/composite materials symposium. Pullman, WA: Washington State University.

WoodWorks. 2021. Building trends: mass timber: quarterly update + map of U.S. mass timber projects. Washington, DC: Woodworks. https://www.woodworks.org/publications-media/building-trends-mass-timber/

Yang, B.Z.; Seale, R.D.; Shmulsky, R.; Dahlen, R.J.; Wang, X. 2015. Comparison of nondestructive testing methods for evaluating No. 2 southern pine lumber: part A, modulus of elasticity. Wood and Fiber Science. 47(4): 375–384.

Yang, B.Z.; Seale, R.D.; Shmulsky, R.; Dahlen, R.J.; Wang, X. 2017. Comparison of nondestructive testing methods for evaluating No. 2 southern pine lumber: part B, modulus of rupture. Wood and Fiber Science. 49(2): 134–145.